SUPPLEMENTAL MATERIAL

Enhanced NLRP3 Inflammasome Signaling Promotes Atrial Fibrillation

Chunxia Yao, Ph.D,* Tina Veleva, M.D,* Larry Scott Jr., B.S, Shuyi Cao, M.S, Luge Li, B.S, Gong Chen, Ph.D, Prince Jeyabal, Ph.D, Xiaolu Pan, M.S, Katherina M. Alsina, B.A, Issam Abu-Taha, Dr. rer. medic, Shokoufeh Ghezelbash, Ph.D, Corey L. Reynolds, Ph.D, Ying H. Shen, M.D, Ph.D, Scott A. LeMaire, M.D, Wilhelm Schmitz, M.D, Frank U. Müller, Ph.D, Ali El-Armouche, M.D, N. Tony Eissa, M.D, Christine Beeton, Ph.D, Stanley Nattel, M.D, Xander H.T. Wehrens, M.D, Ph.D, Dobromir Dobrev, M.D, Na Li, Ph.D

* These authors contributed equally to the manuscript.

Supplemental Methods

Human atrial samples. Right atrial appendages of patients undergoing open-heart surgery for coronary bypass grafting and/or valve replacement were collected with patients' written informed consent. All experimental protocols were approved by the ethics committees of the Medical Faculty Mannheim, University Heidelberg (No. 2011-216N-MA) and Carl Gustav Carus Medical Faculty, Dresden University of Technology (No. EK790799) performed in accordance with the Declaration of Helsinki. After excision, atrial appendages were snap-frozen in liquid-nitrogen for biochemical studies. Patient demographics and characteristics are listed in **Table S1**.

Animal studies. All studies involving mice were performed according to protocols approved by the Institutional Animal Care and Use Committee at Baylor College of Medicine, and conformed to the *Guide for the Care and Use of Laboratory Animals* published by the U.S. National Institutes of Health. NLRP3 homozygous knockout mice ($Nlrp3^{-/-}$)[1] and CREM-IbΔC-X (CREM) TG mice[2-4] were established

previously. CREM-TG mice were crossbred to Nlrp3$^{-/-}$ and the offspring maintained expected Mendelian ratios. CREM-TG:Nlrp3$^{-/-}$ mice were maintained on the mixed FVB:Bl6J background, with at least 6 times of outcrossing CREM-TG (FVB background) mice to NLRP3-/- (C57BL6/J background) mice, so that the so that the CREM-TG:Nlrp3$^{-/-}$ mice are more close to the C57BL6/J background. The control WT mice in the current study were the littermates within the CREM-TG:Nlrp3 colony. To yield mice with cardiomyocyte-specific expression of constitutively active NLRP3, *Myh6*^{Cre} mice were crossbred to Nlrp3$^{neoR\text{-}A350V}$ mice[1] (*Myh6*^{Cre}*:Nlrp3*$^{A350V/+}$). The offspring of this cross also maintained expected Mendelian ratios.

All canine care and handling procedures were in accordance with National Institutes of Health guidelines (http://oacu.od.nih.gov/training/index.htm) and were reviewed and approved by the Animals Research Ethics Committee of The Montreal Heart Institute (Montréal, Quebec). Twenty-six adult mongrel dogs (22 to 36 kg) were divided into 2 groups: control (n=12) and 1-week atrial tachycardia pacing (ATP, n=14). Under diazepam (0.25 mg/kg IV), ketamine (5.0 mg/kg IV), and halothane (1% to 2%) anesthesia, unipolar leads were inserted into the right ventricular apex and right atrial (RA) appendage and connected to pacemakers in the neck. Atrioventricular block was created by radiofrequency ablation, and the right ventricle pacemaker was programmed to 80 bpm. After 24-hour recovery, the atrial pacemaker was programmed to pace the RA appendage at 400 bpm for 7 days. On study days, dogs were anesthetized with morphine (2 mg/kg SC) and α-chloralose (120 mg/kg IV load at 29.25 mg/kg per hour) and ventilated mechanically. Atrial effective refractory periods (AERPs) of RA appendage were determined with 8 basic stimuli followed by 1 premature stimulus (5-ms decrements). AF was induced multiple times by burst pacing to determine AF duration in each dog, and mean AF duration was calculated using average individual dog AF duration values. After open chest studies, hearts were excised through a median thoracotomy and immersed in oxygenated Tyrode solution. RA tissue samples were frozen in liquid N_2 for biochemistry studies.

Western blot analysis. Protein extraction and Western blotting were performed as previously described in detail.[3, 5-7] In brief, atrial lysates of humans, canines and mice were subjected to electrophoresis on 5% or 10% acrylamide gels followed by transfer onto polyvinyl difluoride (PVDF) membranes. Primary antibodies against the following target proteins were then used to probe for NLRP3 (mouse: 1:1,000; MA5-16275; ThermoFisher; canine and human: 1:500; NBP1-77080; NOVUS Biologicals), ASC (mouse: 1:1,000; canine and human: 1:250; sc-22514-R; Santa Cruz), Caspase-1 (mouse: 1:1,000; canine and human: 1:100, SC-56036, Santa Cruz), IL-1β (1:1,000; ab9722; Abcam), CD68 (mouse: 1:1,000; canine and human: 1:200; ab201973; Abcam), TLR4 (mouse: 1:1000; canine and human: 1:200; NB100-56566; NOVUS Biologicals), NFκB-p65 (mouse: 1:1000; human: 1:200; NB100-56712; NOVUS Biologicals), phospo-Ser536-NFκB-p65(mouse: 1:1000; human: 1:200; NB100-82088; NOVUS Biologicals), F4/80 (mouse and human: 1:250; ab16911; abcam), calsequestrin (human: 1:2,500; PA1-913; (ABR) Thermo Sc.), and GAPDH (mouse: 1:10,000; MAB-374; Millipore; canine and human: 1:20,000; Mab6C5, HyTest). Membranes were then incubated with secondary anti-mouse or anti-rabbit antibodies conjugated to Alexa-Fluor 680 (Invitrogen Molecular Probes) or IR800Dye (Rockland Immunochemicals), respectively. Signal intensities were quantified using Image J software.

Nuclear and cytoplasmic protein extraction. Nuclear and cytoplasmic protein extraction was performed as previously described.[8] Frozen atrial tissue was cut into small pieces and washed with PBS, followed by centrifugation (500g, 5 minutes) to remove PBS. Atrial tissues were homogenized (10μL buffer for 1 mg tissue) in CE buffer (20 mM NaF, 1 mM Na_3VO_4, 60 mM KCl, 1 mM EDTA, 1 mM EGTA, 2 mM DTT, 10 mM HEPES, pH 7.9). After incubation on ice for 10 minutes, ice-cold 5% NP-40 (1/10 of CE buffer volume) was added to the sample, followed by vortex and incubation on ice for 1 minute. To separate cytoplasmic and nuclear fractions, centrifugation at 1,500g for 5 minutes was performed, and pellet containing intact nucleus was collected as nuclear fraction, while the supernatant was transferred to a separate tube for cytoplasmic fraction. 1) To extract cytoplasmic proteins, the cytoplasmic fraction collected from the last step was centrifuged again at 16,000g for 20 minutes, and the supernatant was collected as cytoplasmic protein fraction. 2) To extract nuclear proteins, the nuclear fraction was washed three times with 1.0 mL CE buffer, followed by centrifugation at 1,500g for 5 min. After removing the supernatant, the pellet was suspended in NE buffer (CE buffer with 20%

glycerol and 420 mmol/L NaCl) with half volume of the initial CE buffer (5 μL for each mg of original atrial tissue), followed by 1-second sonication for three times on ice and centrifugation at 16,000g for 20 min). The supernatant was collected as nuclear protein fraction.

Preparation of mouse bone marrow derived macrophages. Mouse bone marrow was harvested from femurs and tibiae according a previously published protocol.[9] Cells were washed with DMEM and re-suspended in 100 ml DMEM supplemented with 10% FCS, 10% L929 conditioned medium, Penicillin-Streptomycin (100 U/ml, Gibco), Antibiotic-Antimicotic (amount as indicated by supplier Gibco) and 50 μmol/L of β-mercaptoethanol (Sigma–Aldrich). Cells were incubated for one week under regular cell culture conditions prior preparing proteins from cell lysates for Western blotting.[9]

Quantitative real-time PCR. Total RNA was isolated from the atria of 2-month old mice using the Qiagen RNeasy Mini Kit according to the manufacturer's instructions (Qiagen) and cDNAs were generated using the iScript™ cDNA Synthesis Kit (Bio-Rad, Hercules, CA).[3, 5, 10] qPCR was conducted in triplicate in 96-well plates using SYBR Green SuperMix (Quantabio). Relative mRNA transcript levels (normalized to *RPL7*) were calculated using the CT (cycle number) method and are reported as fold change. The sequences of the primers used in the study were: *Nlrp3,* 5'-AGAGCCTACAGTTGGGTGAAATG-3' (forward), 5'-CCACGCCTACCAGGAAATCTC-3' (reverse); *CREM-IbΔC-X, 5'*-TGGAAGTATAACAGCTTCTTTGACA-3' (forward), 5'-CCAGTGGCAGCTGAGCTAAAG-3' (reverse); *Ryr2*, 5'-GCAGTCCCTGTCAGTACGG-3' (forward), 5'-CGTGTCCATAGAGGAGTGTCC-3' (reverse); *Kcna5*, 5'-CAATCAGGGGTCGCACTTCTC-3' (forward), 5'-ACAGTGGTCATAGTGACTACTGC-3' (reverse); *Girk1*, 5'-GCCCAAGAAGAAACGGCAGC-3' (forward), 5'-CAGGGTAGTGAAGAGGTCCG-3' (reverse); *Girk4*, 5'-CCGAGCGGGTCCACAACACC-3' (forward), 5'-TGCCTGCCTAAGCCTGGGGT-3' (reverse); *Cacna1c, 5'*-TCCCGAGCACATCCCTACTC-3' (forward), 5'-ACTGACGGTAGAGATGGTTGC-3' (reverse); *Mef2c*, 5'-

ACGAGGATAATGGATGAGCGT-3' (forward), 5'-ATCAGTGCAATCTCACAGTCG-3' (reverse); *Rcan1,* 5'-CATGCAGCGACAGACACCAC-3' (forward), 5'-GTGGATGGGTGTGTACTCCG-3' (reverse); *L7*, 5'-GAAGCTCATCTATGAGAAGGC-3' (forward), 5'-AAGACGAAGGAGCTGCAGAAC-3' (reverse).

Isolation of mouse atrial cardiomyocytes. Hearts were removed from WT and *Myh6^{Cre}:Nlrp3$^{A350V/+}$* mice during isoflurane anesthesia. After excision, the heart was cannulated and perfused in Langendorff mode with 0 mmol/L-Ca^{2+} Tyrode solution (1-3 minutes, 37°C), followed by Liberase (TH Research Grade, Roche Applied Science) in 0 mmol/L-Ca^{2+} Tyrode at 37°C until digestion was complete. After digestion, to wash out remaining collagenase, the heart was perfused with 5 mL KB solution containing (in mmol/L): 90 KCl, 30 K_2HPO_4, 5 $MgSO_4$, 5 pyruvic acid, 5 β-hydroxybutyric acid, 5 creatine, 20 taurine, 10 glucose, 0.5 EGTA, 5 HEPES, pH 7.2. The atria were dissected and minced in KB solution, gently agitated, then filtered through a 210-μm polyethylene mesh. After settling, atrial cardiomyocytes were stored in KB solution at room temperature until use.

Calcium imaging. Atrial cardiomyocytes were incubated with the Ca^{2+} indicator Fluo-4-AM (2 μmol/L) in KB solution for 30 minutes at room temperature as previously described.[5, 11] Cells were rinsed with normal Tyrode's solution containing 1.8 mmol/L Ca^{2+} for de-esterification and then transferred to a chamber equipped with a pair of electrodes on a confocal microscope (LSM 510, Carl Zeiss). Fluorescence images were recorded in line-scan mode with 1024 pixels per line at 500 Hz. After being paced at 1 Hz (15 ms pulses, 10 V) for at least 2 minutes, only cardiomyocytes showing clear striations and regular response to electrical pulses were selected for further experiments. Once steady-state Ca^{2+} transients were observed, pacing was stopped and Ca^{2+} sparks were counted using SparkMaster.[12]

Immunocytochemistry. Isolated mouse atrial cardiomyocytes (CMs) were placed on glass slides pre-coated with 20ug/ml of laminin (37°C, 30 minutes). After the cells adhered properly, a gentle wash with PBS was applied to remove unattached cells, followed by fixation using 4% PFA, permeabilization

using 0.1% Triton X, and blocking with 10% natural goat serum (NGS) to further prepare cells to receive antibody treatment. PBS washes occurred between steps. After blocking, cells were incubated with primary antibody (1:100 in NGS/BSA) at 4°C overnight. The following day, after washing off excess primary antibody with PBS, cells were incubated with a complimentary secondary antibody for 1 hour at room temperature. Following a quick PBS wash, mounting medium containing a nuclear DAPI stain was applied to each slide and a coverslip was gently placed. The slides were sealed with nail polish and allowed to set for at least 30 minutes prior to imaging. Images were acquired using a Zeiss confocal microscope. Primary antibodies against the following target proteins were used: NLRP3 (1:1,000; MA5-16275; ThermoFisher), and α-Actinin (1:250; A7811; Sigma-Aldrich).

Histology. Whole hearts were excised, washed briefly in normal saline, blotted dry and then fixed in 4% buffered formaldehyde for 48h. Longitudinal 5μm sections were stained with Masson-Trichrome for fibrosis. Fibrosis was quantified as described.[13]

Adeno-associated virus (AAV) production and delivery. The pAAV-stop-GFP vector[14] was a gift from Dr. Matthias Klugmann (University of New South Wales, Australia). The mCherry-tagged shNlrp3 targeting the sequence of ggttctactctatcaaggaca at site 654 of *mus musculus Nlrp3* (NM_145827.3) or scramble sequence were obtained from GeneCopoeia (MD, USA), and were cloned into the Mlu I site of the pAAV-stop-GFP vector to replace the GFP sequence. The adenoviral helper plasmid pAdDeltaF6 (PL-F-PVADF6) and the AAV9 packaging vector pAAV2/9 (PL-T-P0008-R2) were obtained from Puresyn,Inc.. AAV9 were packaged in HEK293T cells by the triple transfection method and purified by two rounds of CsCl density gradient centrifugation as described.[15, 16] At the age of 2 months, CM-KI mice were injected with one dose of AAV9-scramble or AAV9-shNlrp3 virus ($5x10^{11}$ GC/mouse) via retro-orbital route.[17]

Statistical Analysis. For numerical data which were presented as mean ± SEM, two-tailed Student's *t*-test was used for data comparison of two groups with normal distribution; one-way ANOVA and Holm-Sidak's test were used for data comparison of multiple groups with normal distribution; Mann-Whitney and Kruskal-Wallis test followed by Dunn's test were used to compare groups when the data were not normally distributed. Fisher's exact or Chi-squared tests were used to compare categorical data. P-value of less than 0.05 was considered statistically significant.

Supplemental Tables

Table S1. Characteristics of patients used for biochemistry in atrial whole-tissue lysates.

	SR	pAF	cAF
Patients, n	23	11	20
Gender, m/f	20/3	7/4	13/7
Age, y	68.4±2.5	71.8±2.3	70.4±1.7
Body mass index, kg/m^2	27.6±0.9	31.3±2.7	28.2±1.1
CAD, n (%)	13 (56)	4 (36)	3 (15)
AVD/MVD, n (%)	3 (13)	2 (18)	12 (60)
CAD+AVD/MVD, n (%)	7 (30)	5 (55)	5 (25)
Hypertension, n (%)	21 (91)	11 (100)	20 (100)
Diabetes, n (%)[#]	6 (37)	3 (33)	8 (53)
Hyperlipidemia, n (%)[§]	13 (72)	8 (100)	11 (73)
LVEF, %	50.6±4.2	45.9±4.9	51.3±2.5
LA, mm	45.5±4.9	43.3±3.4	51.5±2.7
Digitalis, n (%)	1 (4)	1 (9)	6 (30)
ACE inhibitors, n (%)	12 (52)	8 (88)	11 (55)
AT1 blockers, n (%)	1 (4)	1 (9)	2 (10)
β-Blockers, n (%)	13 (56)	9 (81)	16 (80)
Dihydropyridines, n (%)	5 (21)	3 (27)	6 (20)
Diuretics, n (%)	4 (17)	7 (63)*	13 (65)*
Nitrates, n (%)	2 (8)	1 (9)	5 (25)
Lipid-lowering drugs, n (%)	12 (52)	7 (63)	7 (35)

SR, sinus rhythm as control; pAF, paroxysmal atrial fibrillation; cAF, chronic atrial fibrillation; CAD, coronary artery disease; AVD, aortic valve disease; MVD, mitral valve disease; LVEF, left ventricular ejection fraction; LA, left atrial diameter; ACE, angiotensin converting enzyme; AT, angiotensin receptor; *P<0.05 *versus* SR from Chi-squared test for categorical variables. All other variables were

not significantly different between groups. [†]Data were not available for 7 SR, 2 pAF and 5 cAF. [‡]Data were not available for 5 Ctl, 3 pAF and 5 cAF.

Table S2. Characteristics of patients used for biochemistry in atrial cardiomyocytes.

	SR	pAF	cAF
Patients, n	18	8	15
Gender, m/f	10/8	3/5	5/10
Age, y	69.2±2.3	72.5±1.8	72.0±2.9
Body mass index, kg/m^2	26.6±0.7	27.1±2.0	26.0±0.7
CAD, n (%)	6 (33)	0 (0)	1 (7)
AVD/MVD, n (%)	9 (50)	5 (62)	8 (53)
CAD+AVD/MVD, n (%)	3 (17)	3 (38)	6 (40)
Hypertension, n (%)	16 (89)	6 (75)	10 (67)
Diabetes, n (%)	3 (17)	0 (0)	5 (33)
Hyperlipidemia, n (%)	11 (61)	6 (75)	6 (40)
LVEF, %	59.4±3.1	57.0±5.5	54.7±2.5
LA, mm$^{\#}$	40.3±2.3	48.8±2.5	48.0±2.9
Digitalis, n (%)	0 (0)	2 (25)*	5 (33)*
ACE inhibitors, n (%)	12 (67)	5 (63)	10 (67)
AT1 blockers, n (%)	2 (11)	1 (13)	0 (0)
β-Blockers, n (%)	16 (89)	8 (100)	9 (60)*
Dihydropyridines, n (%)	2 (11)	1 (13)	2 (13)
Diuretics, n (%)	4 (22)	4 (50)	5 (33)
Nitrates, n (%)	1 (6)	0 (0)	2 (13)
Lipid-lowering drugs, n (%)§	11 (61)	3 (60)	3 (25)

SR, sinus rhythm as control; pAF, paroxysmal atrial fibrillation; cAF, chronic atrial fibrillation; CAD, coronary artery disease; AVD, aortic valve disease; MVD, mitral valve disease; LVEF, left ventricular ejection fraction; LA, left atrial diameter; ACE, angiotensin converting enzyme; AT, angiotensin receptor; *P<0.05 *versus* SR from Chi-squared test for categorical variables. All other variables were not significantly different between groups. †Data were not available for 12 SR, 4 pAF and 12 cAF. ‡Data were not available for 3 pAF and 3 cAF.

Table S3. ECG parameters in cardiomyocyte-specific knockin of NLRP3-A350V (CM-KI) mice.

	CTL (n=13)	CM-KI (n=9)	P-value (CTL vs CM-KI)
RR (ms)	108.6 ± 2.6	106.1 ± 2.9	0.535
HR (bpm)	556.2 ± 13.0	568.9 ± 15.6	0.540
PR (ms)	39.5 ± 0.9	37.3 ± 1.0	0.161
QRS (ms)	9.0 ± 0.3	9.3 ± 0.4	0.491
QTc (ms)	23.2 ± 0.5	23.6 ± 0.8	0.707
SNRT (ms)	133.4 ± 6.5	120.8 ± 3.3	0.051
AVNERP (ms)	48.8 ± 1.5	50.0 ± 1.5	0.585

SNRT, sinus node recovery time; AVNERP, atrioventricular node effective refractory period.

Table S4. Ventricular function in cardiomyocyte-specific knockin of NLRP3-A350V (CM-KI) mice.

	CTL (n=9)	CM-KI (n=4)	P-value (CTL vs CKI)
ESD (mm)	2.27 ± 0.13	3.11 ± 0.19	0.004
EDD (mm)	3.80 ± 0.11	4.24 ± 0.20	0.068
EF (%)	71.7 ± 2.30	52.5 ± 2.49	0.002
Cardiac output (mL/min)	22.2 ± 1.02	17.9 ± 1.68	0.045
LVAWs (mm)	1.84 ± 0.05	1.07 ± 0.02	0.001
LVAWd (mm)	1.25 ± 0.05	1.00 ± 0.02	0.011
LVPWs (mm)	1.49 ± 0.06	1.25 ± 0.26	0.021
LVPWd (mm)	1.01 ± 0.05	0.92 ± 0.03	0.333

EDD, end-diastolic diameter; ESD, end-systolic diameter; EF, ejection fraction; LVAWd, left-ventricular end-diastolic anterior wall thickness; LVAWs, left-ventricular end-systolic anterior wall thickness; LVPWd, left-ventricular end-diastolic posterior wall thickness; LVPWs, left-ventricular end-systolic posterior wall thickness.

Supplemental Figures and Figure Legends

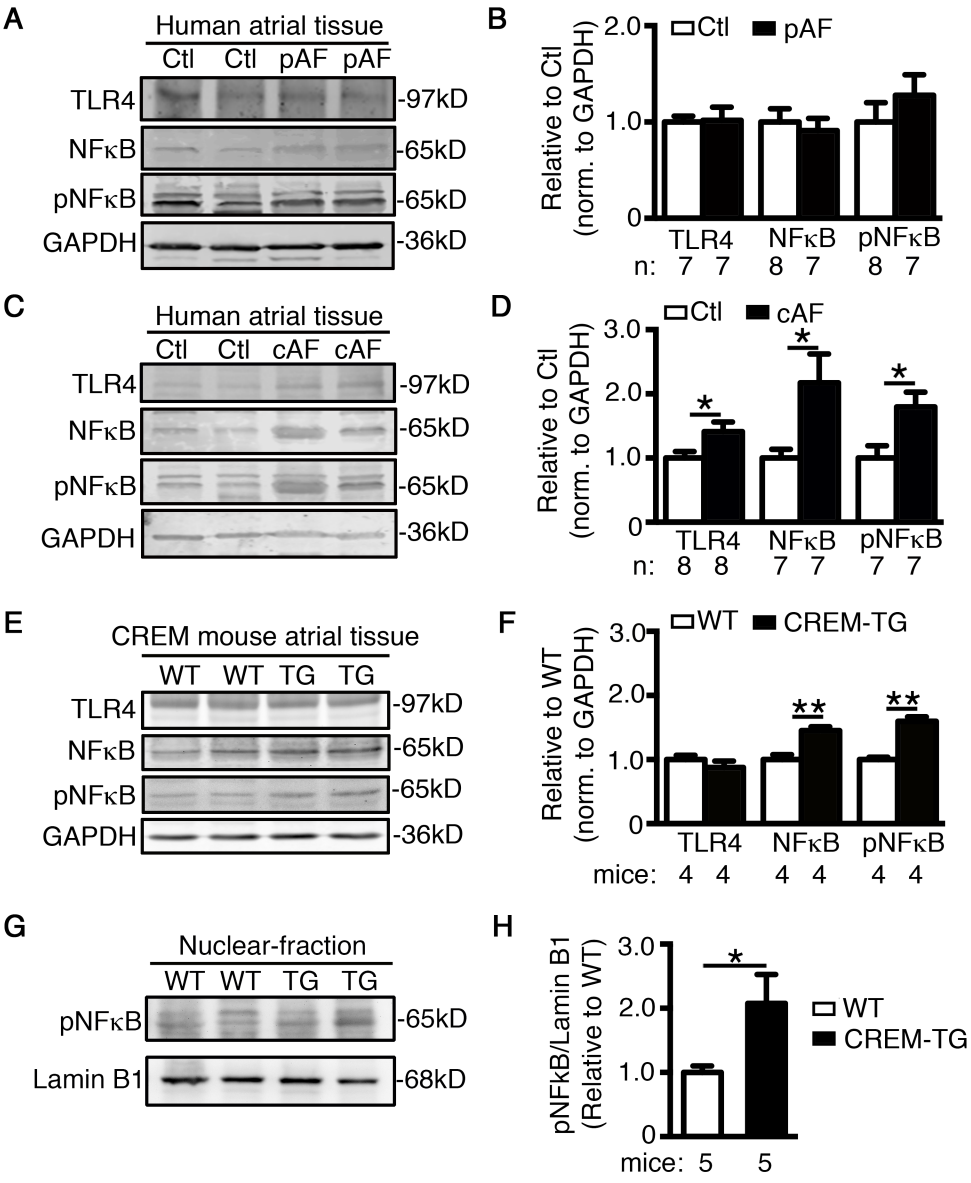

Figure S1. Enhanced activity of TLR4-NFκB pathway in chronic AF (cAF) but not in paroxysmal AF (pAF) patients. (**A, B**) Representative Western blots (WBs) and quantification of TLR4, NFκB, and phosphorylated NFκB (pNFκB) in atrial tissues of patients with pAF and normal sinus rhythm as control (Ctl). (**C, D**) Representative WBs and quantification of TLR4, NFκB, and pNFκB in atrial tissues of patients with cAF and normal sinus rhythm as control (Ctl). (**E, F**) Representative WBs and quantification of TLR4, NFκB, and pNFκB in atrial tissues of CREM-TG mice and WT littermates.

(**G, H**) Representative WBs and quantification of pNFκB and Lamin B1 (the nuclear envelope marker) in the nuclear fraction of atrial tissues of WT and CREM-TG mice. *P<0.05, **P<0.01.

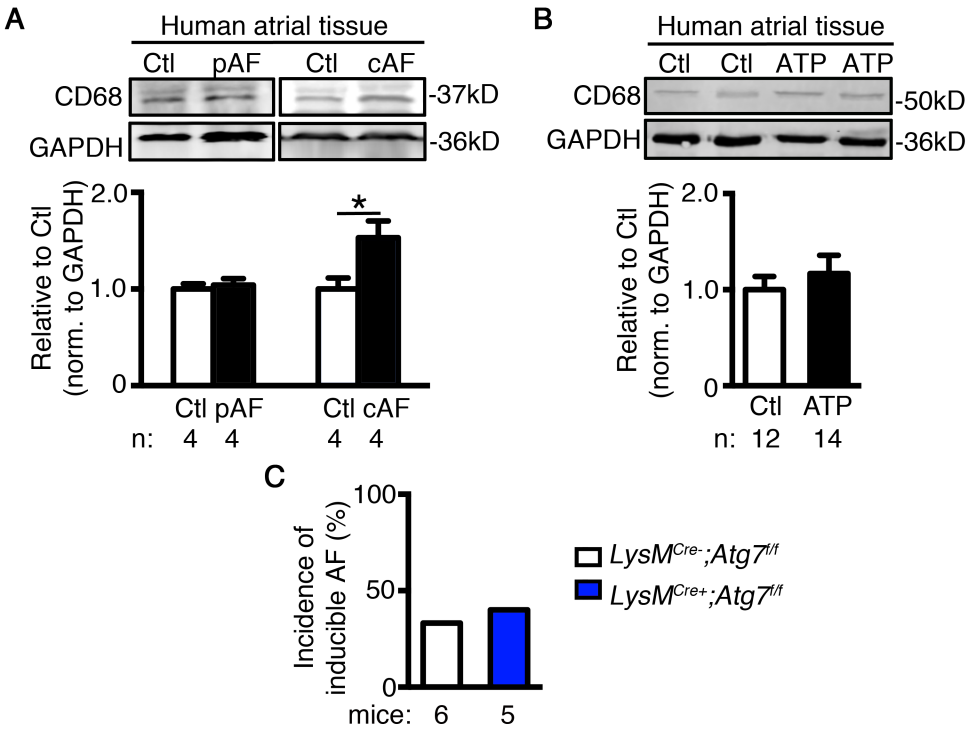

Figure S2. (**A**) Representative WBs and quantification of CD68 (a macrophage marker) in atrial tissues of pAF and cAF patients, respectively, compared to the Ctl samples. (**B**) Representative WBs and quantification of CD68 in atrial tissues of ATP dogs, compared to the Ctl (sham) dogs. *P<0.05 (**C**) Incidence of inducible AF in macrophage-specific autophagy-related 7 knockout mice (*LysM*$^{Cre+}$;*Atg7*$^{f/f}$) and control littermates (*LysM*$^{Cre-}$;*Atg7*$^{f/f}$).

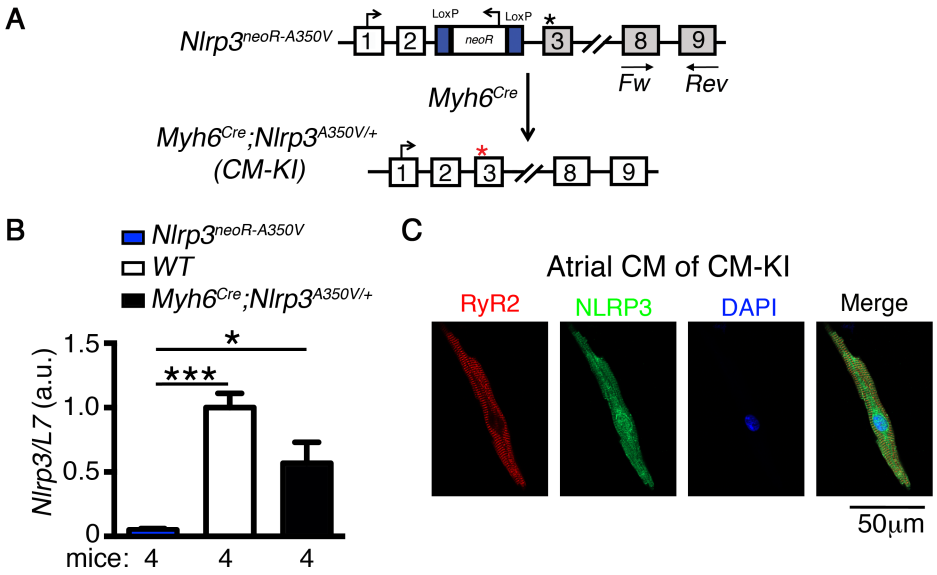

Figure S3. Establishment of cardiomyocyte (CM)-specific knockin model of NLRP3. (**A**) Schematic representation of the transgenic approach used to establish *Myh6*^{Cre}*;Nlrp3*$^{A350V/+}$ (CM-KI) mouse model, and qPCR primers designed to determine the level of *Nlrp3* mRNA. (**B**) qPCR confirmed the re-expression of Nlrp3 in the CM-fraction of CM-KI mice, compared to *Nlrp3*$^{neoR-A350V}$ and wildtype (WT) mice. (**C**) Immunocytochemistry study confirmed the re-expression of NLRP3 in atrial CM of CM-KI mice. *P<0.05, ***P<0.001.

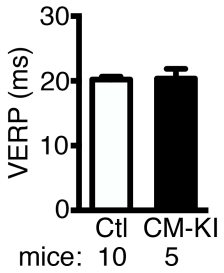

Figure S4. Comparable ventricular-effective-refractory-period (VERP) in *Myh6^{Cre};Nlrp3$^{A350V/+}$* (CM-KI) and Ctl mice (including 5 wildtype and 5 Myh6^{Cre} mice).

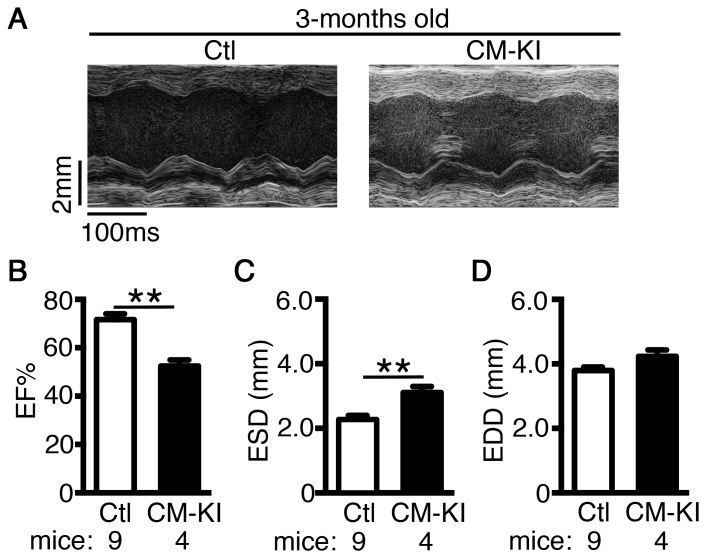

Figure S5. Assessment of cardiac function in CM-KI mice by echocardiography. (**A**) Representative M-mode echocardiography recordings of control (Ctl) and *Myh6*^{Cre}*;Nlrp3*$^{A350V/+}$ (CM-KI) mice at the age of 3-months. The Ctl group included 5 wildtype and 4 Myh6^{Cre} mice. Quantification of ejection fraction (EF%, **B**), end-systolic diameter (ESD, **C**), and end-diastolic diameter (EDD, **D**). **P<0.01.

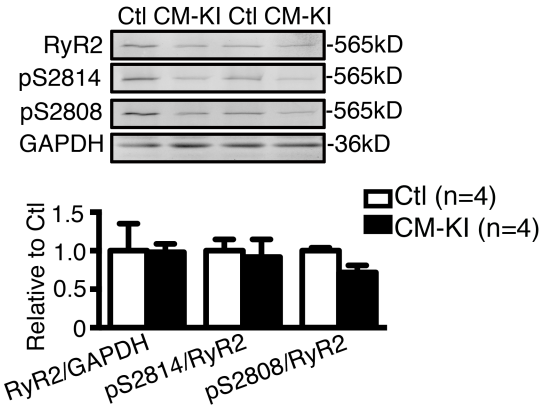

Figure S6. Representative Western blots and quantification demonstrated similar levels of total RyR2 and phosphorylated RyR2 proteins in ventricles of *Myh6*^{Cre}*;Nlrp3*$^{A350V/+}$ (CM-KI) and Ctl mice.

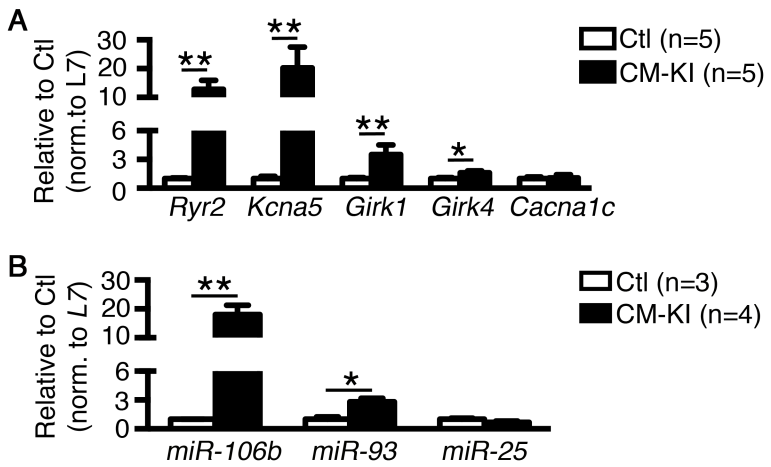

Figure S7. (A) qPCR revealed enhanced transcription of *Ryr2, Kcna5, Girk1,* and *Girk4,* but not *Cacna1c* in atrial tissues of CM-KI compared to Ctl mice. (**B**) Upregulation of *miR-106b* and *miR-93* excludes the contribution of posttranscriptional regulation to the increased level of *Ryr2* mRNA. *P<0.05, **P<0.01.

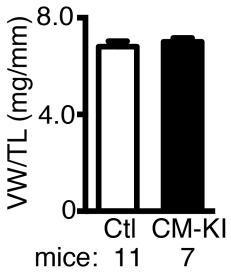

Figure S8. The ratio of ventricular weight to tibia length (VW/TL) was comparable between *Myh6*^{Cre}*;Nlrp3*$^{A350V/+}$ (CM-KI) and Ctl mice (including 6 wildtype and 5 Myh6^{Cre} mice).

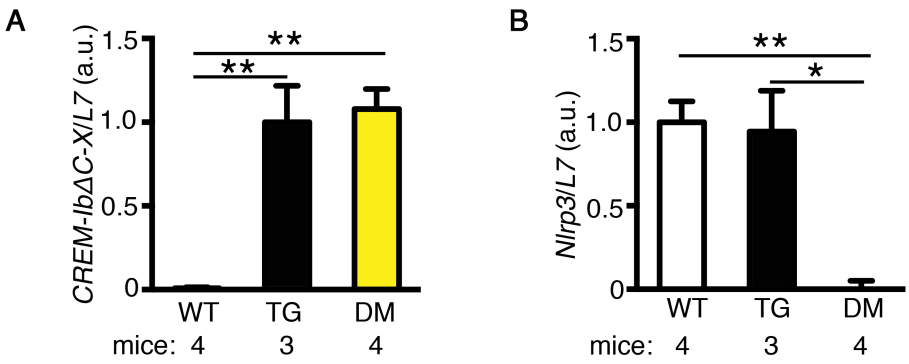

Figure S9. Genetic inhibition of NLRP3 in CREM-TG mice. mRNA level of *CREM-IbΔC-X* (**A**) and *Nlrp3* (**B**) in atrial tissue of WT, CREM-TG, and CREM-TG:NLRP3$^{-/-}$ (DM) mice. *P<0.05, **P<0.01.

Supplemental Reference

1. Brydges SD, Mueller JL, McGeough MD, Pena CA, Misaghi A, Gandhi C, Putnam CD, Boyle DL, Firestein GS, Horner AA, Soroosh P, Watford WT, O'Shea JJ, Kastner DL, Hoffman HM. Inflammasome-mediated disease animal models reveal roles for innate but not adaptive immunity. *Immunity*. 2009;30:875-887. doi:10.1016/j.immuni.2009.05.005
2. Kirchhof P, Marijon E, Fabritz L, Li N, Wang W, Wang T, Schulte K, Hanstein J, Schulte JS, Vogel M, Mougenot N, Laakmann S, Fortmueller L, Eckstein J, Verheule S, Kaese S, Staab A, Grote-Wessels S, Schotten U, Moubarak G, Wehrens XH, Schmitz W, Hatem S, Muller FU. Overexpression of cAMP-response element modulator causes abnormal growth and development of the atrial myocardium resulting in a substrate for sustained atrial fibrillation in mice. *Int J Cardiol*. 2013;166:366-374. doi:10.1016/j.ijcard.2011.10.057
3. Li N, Chiang DY, Wang S, Wang Q, Sun L, Voigt N, Respress JL, Ather S, Skapura DG, Jordan VK, Horrigan FT, Schmitz W, Muller FU, Valderrabano M, Nattel S, Dobrev D, Wehrens XH. Ryanodine receptor-mediated calcium leak drives progressive development of an atrial fibrillation substrate in a transgenic mouse model. *Circulation*. 2014;129:1276-1285. doi:10.1161/CIRCULATIONAHA.113.006611
4. Muller FU, Lewin G, Baba HA, Boknik P, Fabritz L, Kirchhefer U, Kirchhof P, Loser K, Matus M, Neumann J, Riemann B, Schmitz W. Heart-directed expression of a human cardiac isoform of cAMP-response element modulator in transgenic mice. *J Biol Chem*. 2005;280:6906-6914. doi:10.1074/jbc.M407864200
5. Chiang DY, Kongchan N, Beavers DL, Alsina KM, Voigt N, Neilson JR, Jakob H, Martin JF, Dobrev D, Wehrens XH, Li N. Loss of microRNA-106b-25 cluster promotes atrial fibrillation by enhancing ryanodine receptor type-2 expression and calcium release. *Circ Arrhythm Electrophysiol*. 2014;7:1214-1222. doi:10.1161/CIRCEP.114.001973

6. Voigt N, Heijman J, Wang Q, Chiang DY, Li N, Karck M, Wehrens XH, Nattel S, Dobrev D. Cellular and molecular mechanisms of atrial arrhythmogenesis in patients with paroxysmal atrial fibrillation. *Circulation*. 2014;129:145-156. doi:10.1161/CIRCULATIONAHA.113.006641

7. Voigt N, Li N, Wang Q, Wang W, Trafford AW, Abu-Taha I, Sun Q, Wieland T, Ravens U, Nattel S, Wehrens XH, Dobrev D. Enhanced sarcoplasmic reticulum Ca2+ leak and increased Na+-Ca2+ exchanger function underlie delayed afterdepolarizations in patients with chronic atrial fibrillation. *Circulation*. 2012;125:2059-2070. doi:10.1161/CIRCULATIONAHA.111.067306

8. Morin S, Charron F, Robitaille L, Nemer M. GATA-dependent recruitment of MEF2 proteins to target promoters. *EMBO J*. 2000;19:2046-2055. doi:10.1093/emboj/19.9.2046

9. Chebrolu C, Artner D, Sigmund AM, Buer J, Zamyatina A, Kirschning CJ. Species and mediator specific TLR4 antagonism in primary human and murine immune cells by betaGlcN(1<-->1)alphaGlc based lipid A mimetics. *Mol Immunol*. 2015;67:636-641. doi:10.1016/j.molimm.2015.07.037

10. Chiang DY, Zhang M, Voigt N, Alsina KM, Jakob H, Martin JF, Dobrev D, Wehrens XH, Li N. Identification of microRNA-mRNA dysregulations in paroxysmal atrial fibrillation. *Int J Cardiol*. 2015;184C:190-197. doi:10.1016/j.ijcard.2015.01.075

11. Li N, Wang T, Wang W, Cutler MJ, Wang Q, Voigt N, Rosenbaum DS, Dobrev D, Wehrens XH. Inhibition of CaMKII phosphorylation of RyR2 prevents induction of atrial fibrillation in FKBP12.6 knockout mice. *Circ Res*. 2012;110:465-470. doi:10.1161/CIRCRESAHA.111.253229

12. Picht E, Zima AV, Blatter LA, Bers DM. SparkMaster: automated calcium spark analysis with ImageJ. *Am J Physiol Cell Physiol*. 2007;293:C1073-1081. doi:10.1152/ajpcell.00586.2006

13. Dahab GM, Kheriza MM, El-Beltagi HM, Fouda AM, El-Din OA. Digital quantification of fibrosis in liver biopsy sections: description of a new method by Photoshop software. *J Gastroenterol Hepatol*. 2004;19:78-85. doi:3183 [pii]

14. Guggenhuber S, Monory K, Lutz B, Klugmann M. AAV vector-mediated overexpression of CB1 cannabinoid receptor in pyramidal neurons of the hippocampus protects against seizure-induced excitoxicity. *PLoS One*. 2010;5:e15707. doi:10.1371/journal.pone.0015707

15. Jarrett KE, Lee CM, Yeh YH, Hsu RH, Gupta R, Zhang M, Rodriguez PJ, Lee CS, Gillard BK, Bissig KD, Pownall HJ, Martin JF, Bao G, Lagor WR. Somatic genome editing with CRISPR/Cas9 generates and corrects a metabolic disease. *Sci Rep*. 2017;7:44624. doi:10.1038/srep44624

16. Lagor WR, Johnston JC, Lock M, Vandenberghe LH, Rader DJ. Adeno-associated viruses as liver-directed gene delivery vehicles: focus on lipoprotein metabolism. *Methods Mol Biol*. 2013;1027:273-307. doi:10.1007/978-1-60327-369-5_13

17. Yardeni T, Eckhaus M, Morris HD, Huizing M, Hoogstraten-Miller S. Retro-orbital injections in mice. *Lab Anim (NY)*. 2011;40:155-160. doi:10.1038/laban0511-155